EUROPEAN JOURNAL OF PURE AND APPLIED MATHEMATICS
2025, Vol. 18, Issue 3, Article Number 6376
ISSN 1307-5543 – ejpam.com
Published by New York Business Global

A Novel U-Statistic Test for Exponentiality Against EBUCL Reliability Class and Applied to Complete and Censored Data Across Various Risk Profiles

Walid B. H. Etman[1], Mohamed F. Abouelenein[2], Mohamed S. Eliwa[3,4], Mahmoud El-Morshedy[5,6,*], Noura Roushdy[2], Rashad M. EL-Sagheer[7,8]

[1] *Faculty of Computer and Artificial Intelligence, Modern University for Technology and Information, Cairo, Egypt*
[2] *Department of Insurance and Risk Management, College of Business, Imam Mohammad Ibn Saud Islamic University (IMSIU), Riyadh 11432, Riyadh, Saudi Arabia*
[3] *Department of Statistics and Operations Research, College of Science, Qassim University, Saudi Arabia*
[4] *Department of Mathematics, Faculty of Science, Mansoura University, Mansoura 35516, Egypt.*
[5] *Department of Mathematics, College of Science and Humanities in Al-Kharj, Prince Sattam bin Abdulaziz University, Al-Kharj 11942, Saudi Arabia*
[6] *Department of Statistics and Computer Science, Faculty of Science, Mansoura University, Mansoura 35516, Egypt*
[7] *Mathematics Department, Faculty of Science, Al-Azhar University, Naser city 11884, Cairo, Egypt*
[8] *High Institute of Computer and Management Information System, First Statement, New Cairo 11865, Cairo, Egypt*

Abstract. Statistical testing plays a pivotal role in enabling researchers to draw sound conclusions from data. Nonparametric tests, in particular, are highly valuable due to their flexibility in handling various data sets without requiring assumptions about the underlying distribution. In response to the growing need for robust testing procedures, this study introduces a new class of life distributions known as exponential better than used in convex Laplace transform order (EBUCL). A novel U-statistic-based test is developed to evaluate exponentiality against this class. The asymptotic properties of the proposed test are thoroughly examined, and critical values for sample sizes ranging from 5 to 50 are reported. A detailed simulation study evaluates the test's power under commonly encountered reliability models. Moreover, Pitman's asymptotic efficiency is calculated and compared with that of existing methods. The study also extends the methodology to handle right-censored data. Finally, the practical utility of the proposed test is demonstrated through applications to several real-world data sets from diverse fields.
2020 Mathematics Subject Classifications: 62N01, 62N02, 62N05, 62C07, 62G99
Key Words and Phrases: Nonparametric Statistics, Ageing Classifications in Reliability, Failure Analysis, Asymptotic Test Efficiency, Decision Support Systems

*Corresponding author.
DOI: https://doi.org/10.29020/nybg.ejpam.v18i3.6376

Email address: m.elmorshedy@psau.edu.sa (Mahmoud El-Morshedy)

1. Introduction

The integration of sustainability-driven analysis with censored data within the framework of reliability aging classes of life distributions represents a critical advancement in the understanding of product durability and lifespan. This integration not only enhances our ability to assess product performance over time but also plays a crucial role in informing decision-making related to resource management, environmental impact, and the evolution of sustainable methodologies. By analyzing censored data, which is often prevalent in real-world scenarios where full lifetime information is unavailable, researchers can derive valuable insights into the reliability and resilience of products. These insights are fundamental for evaluating how products perform under varying conditions and contribute to their overall longevity. Moreover, this integrated analytical approach equips decision-makers with the tools needed to assess environmental footprints and develop strategies to mitigate adverse impacts. By examining the relationships between product durability, reliability, and sustainability, this method supports the creation of eco-conscious strategies and promotes the adoption of sustainable practices across industries. Through comprehensive statistical analyses, this approach not only provides a clearer picture of product reliability but also lays the foundation for the development of robust sustainability frameworks. These frameworks are essential for improving resource efficiency, reducing waste, and advancing responsible environmental stewardship.

Reliability, as a concept, is central to ensuring that products and systems consistently meet performance standards over time. It is defined as the ability to replicate measurements consistently, which is crucial for developing reliable tests and analyses. Inconsistent outcomes undermine the effectiveness of any test, preventing valid comparisons between data sets. While reliability ensures consistency, validity assesses the accuracy of measurements, and the two concepts are distinct. A test may be reliable, consistently producing results, but still lack validity if those results are not accurate.

In industrial engineering, reliability is paramount. It denotes a system's ability to perform its intended task effectively over time, with minimal failure. Given that modern products often consist of multiple interconnected components, the risk of failure increases if any individual part malfunctions. Therefore, a product is deemed reliable when it consistently performs its functions throughout its expected lifespan. The core of reliability theory is built upon the principles of measuring, analyzing, and evaluating the performance of products and systems, ensuring that they meet both operational and longevity standards.

In fields such as probability, statistics, economics, survival analysis, and reliability theory, key concepts such as symmetry, asymmetry, and stochastic comparison of probability distributions are integral to the analysis. Symmetry and asymmetry are particularly significant in reliability analysis, where asymmetric data present greater challenges for prediction compared to symmetric data. Asymmetric distributions, often seen in real-world reliability data, can complicate model building but also provide opportunities to identify outliers or anomalies that may indicate potential system failures. On the other hand, symmetric distributions, with their more predictable patterns, can enhance the accuracy and

efficiency of predictive models. Understanding the role of both symmetry and asymmetry is essential for developing effective strategies to predict and improve reliability, particularly in complex systems with multiple interacting components. Among the numerous life distribution types studied, the exponential distribution stands out, as an example, EL-Sagheer et al. [1], Navarro and Pellerey [2], Ghosh and Mitra [3], Bakr and Al-Babtain [4], Alqifar et al. [5], Bryson and Siddiqui [6], Barlow and Proschan [7], El-Morshedy et al. [8], Gadallah et al. [9], Mansour [10], Klefsjo [11], Kumazawa [12], Abu-Youssef et al. [13], Mahmoud and Mansour [14], Bakr [15] and Qaid et al. [16]. This distribution finds applications in various fields: estimating distances between DNA mutations (Duan et al. [17]), predicting radioactive particle decay (Poston [18]), determining molecule heights in a gas under specific conditions (Beckers et al. [19]), modeling rainfall and river flow volumes (Tomy et al. [20]). Elbatal [21] introduced a class of life distribution termed *exponential better than used* (EBU) and its counterpart class *exponential worse than used* (EWU), exploring their relationships with different life distribution groups. Elbatal investigated closure qualities under the shock model, moment inequality, and reliability operations within these classes. Some of the fundamental definitions that made it easier to derive our class include the following:

Definition (1): A random variable X is said to be

(i) *Exponential better than used*, denoted by $X \in EBU$, if

$$\overline{F}(x+t) \leq \overline{F}(t)\, e^{\frac{-x}{\mu}}, \quad x,t>0.$$

(ii) *Exponential better than used in increasing convex order*, denoted by $X \in EBUC$, if

$$\int_u^{\infty} \overline{F}(x+t)\, dx \leq \mu e^{\frac{-x}{\mu}} \overline{F}(t), \quad x,t>0,$$

or

$$\int_{x+t}^{\infty} \overline{F}(u)\, dx \leq \mu e^{\frac{-x}{\mu}} \overline{F}(t),$$

and this leads to

$$\mu \overline{W}_F(x+t) \leq \mu e^{\frac{-x}{\mu}} \overline{F}(t),$$

such that $\overline{W}_F(x+t) = \frac{1}{\mu}\int_{x+t}^{\infty} \overline{F}(u)du$

$$\overline{W}_F(x+t) \leq e^{\frac{-x}{\mu}} \overline{F}(t).$$

(iii) *Exponential better than used in increasing convex in Laplace transform order*, denoted by $X \in EBUCL$, if

$$\int_0^{\infty} e^{-sx} \overline{W}_F(x+t)\, dx \leq (\geq) \overline{F}(t) \int_0^{\infty} e^{-sx} e^{\frac{-x}{\mu}} dx, \quad x,t>0, s \geq 0,$$

or

$$\int_0^{\infty} e^{-sx} \overline{W}_F(x+t)\, dx \leq (\geq) \frac{\mu}{\mu s+1} \overline{F}(t), \quad x,t>0, s \geq 0.$$

Remark 1. It is clear that
$$\begin{array}{ccccc} \text{NBU} & \subset & \text{NBUE} & \subset & \text{HNBUE.} \\ \cap & & \cup & & \\ \text{EBU} & \subset & \text{EBUC} & \subset & \text{EBUCL.} \end{array}$$

Where: *New better than used* (NBU), *New better than used in expectation* (NBUE), and *Harmonic new better than used in expectation* (HNBUE).

1.1. Motivation and relevance

The primary aim of this study is to address the current limitations in the efficiency and power of nonparametric tests for life distributions. Existing methods often fall short in terms of both test power and efficiency, motivating the development of a novel class of life distributions that improves upon these aspects. Specifically, we introduce a new class that enhances both test effectiveness and power. In contrast to previous work, where distinct classes and exponential tests have been explored (e.g., the NBRULC class in reference [8] with Moment Inequality-based testing and the EBU class in reference [21] with U-statistic-based testing), the proposed class offers a more robust framework for assessing exponentiality. This distinction highlights the novelty and potential of our approach for advancing nonparametric testing.

1.2. Outline of the paper

This paper begins by highlighting the limitations of existing nonparametric tests for life distributions, specifically in terms of test efficiency and power. The primary aim is to introduce a novel class of life distributions, the EBUCL class, and develop a U-statistic-based test for exponentiality against this class. The theoretical contribution is the establishment of a framework that links Laplace transform ordering with ageing concepts in reliability theory. The methodological innovation includes the derivation of a U-statistic test that exhibits desirable properties such as unbiasedness and asymptotic normality, with a derived asymptotic null distribution for both complete and censored data. The computational study presents Monte Carlo simulations, which demonstrate the superior empirical power of the proposed test compared to existing methods. Additionally, Pitman's asymptotic efficiency is computed and compared with other tests to highlight its efficiency and sensitivity to alternative distributions. The paper then applies the proposed test to real-world datasets from engineering, biostatistics, and actuarial science, showcasing its practical value. Finally, the test's extension to right-censored data broadens its utility, with an emphasis on the handling of incomplete data, a common occurrence in reliability studies.

2. Assessing Alternatives to EBUCL through Testing

In contrast to the associated hypothesis $H_1 : F$ suggesting non-exponential behavior but $EBUCL$, this section investigates the potential scenario where $H_0 : F$ represents exponentiality. The theorem presented herein serves as the basis for deriving the test statistic.

Theorem 1.
Suppose there exists an $EBUCL$ random variable X with a distribution function F, thus

$$\frac{\mu^2}{\mu s+1} \geq \frac{1}{2s}\mu_{(2)} - \frac{1}{s^3}\phi(s) - \frac{1}{s^2}\mu + \frac{1}{s^3}, s \geq 0. \tag{1}$$

where

$$\phi(s) = Ee^{-sX} = \int_0^\infty e^{-sx} dF(x).$$

Proof.
Since F is $EBUCL$ then

$$\int_0^\infty e^{-sx}\overline{W}_F(x+t)\,dx \leq \frac{\mu}{\mu s+1}\overline{F}(t), \quad x,t \geq 0.$$

Upon integrating both sides across the interval $[0,\infty)$ with respect to t, the result is

$$\int_0^\infty \int_0^\infty e^{-sx}\overline{W}_F(x+t)\,dxdt \leq \frac{\mu^2}{\mu s+1}. \tag{2}$$

Setting

$$\begin{aligned}
I &= \int_0^\infty \int_0^\infty e^{-sx}\overline{W}_F(x+t)\,dxdt \\
&= E\int_0^\infty \int_0^\infty e^{-sx}(X-x-t)I(X>x+t)I(X>t)dxdt \\
&= E\int_0^X \int_0^{X-t} e^{-sx}(X-x-t)dxdt \\
&= E\int_0^X \int_0^{X-t} \left[Xe^{-sx} - xe^{-sx} - te^{-sx}\right]dxdt \\
&= E\int_0^X \left[\frac{1}{s}X + \frac{1}{s^2}e^{-sX}e^{st} - \frac{1}{s^2} - \frac{1}{s}t\right]dt,
\end{aligned}$$

therefore,

$$I = \frac{1}{2s}\mu_{(2)} - \frac{1}{s^3}\phi(s) - \frac{1}{s^2}\mu + \frac{1}{s^3}. \tag{3}$$

Substituting (3) into (2), we get

$$\frac{\mu^2}{\mu s+1} \geq \frac{1}{2s}\mu_{(2)} - \frac{1}{s^3}\phi(s) - \frac{1}{s^2}\mu + \frac{1}{s^3}.$$

This completes the proof. Allow the measure of deviation from exponentiality to be suggested as follows: By setting

$$\delta(s) = \frac{1}{s^2}\mu\phi(s) + \frac{1}{s^3}\phi(s) - \frac{1}{2}\mu\mu_{(2)} - \frac{1}{2s}\mu_{(2)} + (\frac{1}{s}+1)\mu^2 - \frac{1}{s^3}. \tag{4}$$

Note that under $H_0, \delta(s) = 0$, while under $H_1, \delta(s) > 0$. Let $X_1, X_2, ..., X_n$ be a random sample from a distribution F, the empirical estimate $\hat{\delta}(s)$ of $\delta(s)$ can be obtained as

$$\hat{\delta}(s) = \frac{1}{n^2}\sum_{i=1}^{n}\sum_{j=1}^{n}\left\{\frac{1}{s^2}X_i e^{-sX_j} + \frac{1}{s^3}e^{-sX_i} - \frac{1}{2}X_i X_j^2 - \frac{1}{2s}X_i^2 + \left(\frac{1}{s}+1\right)X_i X_j - \frac{1}{s^3}\right\}.$$

Based on Maclaurin series $\left(e^{-X} = 1 - X + \frac{X^2}{2!} - \frac{X^3}{3!} + ... + (-1)^n \frac{X^n}{n!} + ..\right)$, we get

$$\frac{1}{s^2}X_i e^{-sX_j} + \frac{1}{s^3}e^{-sX_i} - \frac{1}{2}X_i X_j^2 - \frac{1}{2s}X_i^2 + \left(\frac{1}{s}+1\right)X_i X_j - \frac{1}{s^3} = X_1 X_2 - \frac{1}{2}X_1 X_2^2 - \frac{1}{2s}X_1^2.$$

To make the test invariant, let $\Delta(s) = \frac{\delta(s)}{\mu^3}$ which estimated by $\hat{\Delta}(s) = \frac{\hat{\delta}(s)}{\overline{X}^3}$ where $\overline{X}$ is the sample mean. Then

$$\hat{\Delta}(s) = \frac{1}{n^2\overline{X}^3}\sum_{i=1}^{n}\sum_{j=1}^{n}\left\{\frac{1}{s^2}X_i e^{-sX_j} + \frac{1}{s^3}e^{-sX_i} - \frac{1}{2}X_i X_j^2 - \frac{1}{2s}X_i^2 + \left(\frac{1}{s}+1\right)X_i X_j - \frac{1}{s^3}\right\}. \tag{5}$$

One can note that $\hat{\Delta}(s)$ is an unbiased estimator of $\delta(s)$. It is easy to show that: $E(\hat{\Delta}(s)) = \Delta(s)$. Now, set

$$\phi(X_i, X_j) = \frac{1}{s^2}X_i e^{-sX_j} + \frac{1}{s^3}e^{-sX_i} - \frac{1}{2}X_i X_j^2 - \frac{1}{2s}X_i^2 + \left(\frac{1}{s}+1\right)X_i X_j - \frac{1}{s^3}, \tag{6}$$

and define the symmetric kernel

$$\psi_s(X_i, X_j) = \frac{1}{2!}\sum \phi_s(X_i, X_j),$$

where the U_n-statistic provided by is equal to $\hat{\Delta}(s)$ in (5) where the summation over all arrangements of X_i, X_j

$$U_n = \frac{1}{\binom{n}{2}}\sum_{i<j}^{n}\psi_s(X_i, X_j). \tag{7}$$

The following theorem outlines the test's asymptotic properties.

Theorem 2.

(i) As $n \to \infty, \sqrt{n}(\hat{\Delta}(s) - \Delta(s))$ is asymptotically normal with mean 0 and variance $\sigma^2(s)$, where $\sigma^2(s)$ is given by

$$\begin{aligned}\sigma^2(s) = Var\{&\frac{1}{s^2}XE(e^{-sX}) + \frac{1}{s^3}e^{-sX} - \frac{1}{2}XE(X^2) - \frac{1}{2s}X^2 + (\frac{1}{s}+1)XE(X) + \frac{1}{s^2}E(X)e^{-sX} \\ &+ \frac{1}{s^3}E(e^{-sX}) - \frac{1}{2}X^2E(X) - \frac{1}{2s}E(X^2) + (\frac{1}{s}+1)XE(X) - \frac{2}{s^3}\}.\end{aligned} \tag{8}$$

(ii) Under H_0, the variance $\sigma_0^2(s)$ is

$$\sigma_0^2(s) = \frac{4s^3 + 14s^2 + 20s + 11}{(1+s)^2(1+2s)}. \tag{9}$$

Proof.
Below are explicit computations to ascertain the mean and variance utilizing Lee [22], a foundational U-statistics theory

$$\sigma^2 = Var\left\{\eta(X)\right\},$$

where

$$\eta(X) = \eta_1(X) + \eta_2(X),$$

$$\eta_1(X) = E\left(\phi(X_1, X_2) \mid X_1\right) = \frac{1}{s^2}X\int_0^\infty e^{-sx}dF(x) + \frac{1}{s^3}e^{-sX} - \frac{1}{2}X\int_0^\infty x^2dF(x) - \frac{1}{2s}X^2 + \left(\frac{1}{s}+1\right)X\int_0^\infty xdF(x) - \frac{1}{s^3},$$

and

$$\eta_2(X) = E(\phi(X_1, X_2) \mid X_2) = \frac{1}{s^2}e^{-sX}\int_0^\infty xdF(x) + \frac{1}{s^3}\int_0^\infty e^{-sx}dF(x) - \frac{1}{2}X^2\int_0^\infty xdF(x) - \frac{1}{2s}\int_0^\infty x^2dF(x) + \left(\frac{1}{s}+1\right)X\int_0^\infty xdF(x) - \frac{1}{s^3}.$$

Therefore,

$$\eta(X) = \frac{1}{s^2}X\int_0^\infty e^{-sx}dF(x) + \frac{1}{s^3}e^{-sX} - \frac{1}{2}X\int_0^\infty x^2dF(x) - \frac{1}{2s}X^2 + \left(\frac{1}{s}+1\right)X\int_0^\infty xdF(x) + \frac{1}{s^2}e^{-sX}\int_0^\infty xdF(x) + \frac{1}{s^3}\int_0^\infty e^{-sx}dF(x) - \frac{1}{2}X^2\int_0^\infty xdF(x) - \frac{1}{2s}\int_0^\infty x^2dF(x) + \left(\frac{1}{s}+1\right)X\int_0^\infty xdF(x) - \frac{2}{s^3}.$$

Upon using (6), Eq (8) can be obtained.

$$\sigma_0^2(s) = Var\left\{\left[\frac{s+1}{s^3}\right]e^{-sX} - \left[\frac{s+1}{2s}\right]X^2 + \left[\frac{s^3+3s^2+2s+1}{s^2(s+1)}\right]X - \left[\frac{s^3+s^2+2s+1}{s^3(s+1)}\right]\right\}.$$

From (8) and after some computations Eq (9) can be aquired.

3. Pitman's Asymptotic Efficiency of $\Delta(s)$

The prevailing method commonly employed to compare the asymptotic performance of multiple tests is known as Pitman efficiency. Pitman's asymptotic efficiency compares two statistical tests based on their sample sizes. It signifies the minimum sample sizes required for each test to achieve a specified level of power and significance, as the alternative hypothesis converges toward the null hypothesis. Tests with higher Pitman's efficiency require fewer observations to attain the same precision as tests with lower efficiency. One

potential application of asymptotic Pitman efficiency involves comparing different tests for various statistical problems to select the most effective one. For instance, it can be used to compare tests for equality of means, variances, or proportions between two populations. Additionally, it can assess tests for independence, regression, or correlation of two variables. By identifying the test that demands the smallest sample size, Pitman efficiency aids in selecting the optimal test for a specific problem. In this section, the evaluation involves Pitman's asymptotic efficiency (PAE) applied to the Makeham, Weibull, and linear failure rate (LFR) distributions using the described probability models. This assessment aims to determine the performance of these distributions through Pitman's asymptotic efficiency approach.

(i) The Weibull distribution: $\overline{F}_1(x) = e^{-x^\theta}, x \geq 0, \theta \geq 1.$

(ii) The linear failure rate distribution (LFR): $\overline{F}_2(x) = e^{-x-\frac{\theta}{2}x^2}, x \geq 0, \theta \geq 0.$

(iii) The Makeham distribution: $\overline{F}_3(x) = e^{-x-\theta\left(x+e^{-x}-1\right)}, x \geq 0, \theta \geq 0.$

Keep in mind that $\overline{F}_1(x)$ reduces to an exponential distribution for $\theta = 1$, whereas $\overline{F}_2(x)$and $\overline{F}_3(x)$ reduce to an exponential distribution for $\theta = 0$. $\hat{\Delta}(s)$'s PAE is determined by

$$PAE(\Delta(s)) = \frac{1}{\sigma_\circ(s)} \left| \frac{d}{d\theta}\Delta(s) \right|_{\theta \to \theta_\circ}. \tag{10}$$

At $s = 0.97$,

$$\delta_\theta(s) = \frac{1}{s^2}\mu_\theta\phi_\theta(s) + \frac{1}{s^3}\phi_\theta(s) - \frac{1}{2}\mu_\theta\mu_{(2\theta)} - \frac{1}{2s}\mu_{(2\theta)} + \left(\frac{1}{s}+1\right)\mu_\theta^2 - \frac{1}{s^3},$$

where

$$\phi_\theta(s) = \int_0^\infty e^{-sx} dF_\theta(x), \mu_{(2\theta)} = 2\int_0^\infty x\overline{F}_\theta(x)dx, \mu_\theta = \int_0^\infty \overline{F}_\theta(x)dx.$$

Hence,

$$\frac{d}{d\theta}\delta_\theta(s) = \frac{1}{s^2}\left[\mu_\theta\phi_\theta^{\backprime}(s) + \mu_\theta^{\backprime}\phi_\theta(s)\right] + \frac{1}{s^3}\phi_\theta^{\backprime}(s) - \frac{1}{2}[\mu_\theta\mu_{(2\theta)}^{\backprime} + \mu_\theta^{\backprime}\mu_{(2\theta)}] - \frac{1}{2s}\mu_{(2\theta)}^{\backprime} + [\frac{2}{s}+2]\mu_\theta\mu_\theta^{\backprime},$$

where

$$\backprime = \frac{d}{d\theta}, \mu_\theta^{\backprime} = \int_0^\infty \overline{F}_\theta^{\backprime}(x)dx, \mu_{(2\theta)}^{\backprime} = 2\int_0^\infty x\overline{F}_\theta^{\backprime}(x)dx, \phi_\theta^{\backprime}(s) = -\int_0^\infty e^{-sx}d\overline{F}_\theta^{\backprime}(x).$$

Upon using the definition of the PAE in (10),we obtain

$$PAE(\delta) = \frac{1}{\sigma_0}\left|\frac{1}{s^2}\left[\mu_\theta\phi_\theta^{\backprime}(s) + \mu_\theta^{\backprime}\phi_\theta(s)\right] + \frac{1}{s^3}\phi_\theta^{\backprime}(s) - \frac{1}{2}[\mu_\theta\mu_{(2\theta)}^{\backprime} + \mu_\theta^{\backprime}\mu_{(2\theta)}] - \frac{1}{2s}\mu_{(2\theta)}^{\backprime} + [\frac{2}{s}+2]\mu_\theta\mu_\theta^{\backprime}\right|_{\theta\to\theta_\circ}.$$

Table 1 shows a comparison between our test $\hat{\Delta}(s)$ and those of Qaid et al. [16] ($\Delta_n(0.05)$), Etman et al. [23] ($\hat{\Delta}(0.9)$) and Abdel-Aziz [24] ($\hat{\Delta}_{RN}$).

Table 1. Compares the PAE test with a few competitor tests.

Distribution	$\Delta_n(0.05)$	$\hat{\Delta}(0.9)$	$\hat{\Delta}_{RN}$	Our test $\hat{\Delta}(s)$		
				$s = 0.97$	$s = 1$	$s = 2$
Weibull	1.203	0.851	0.223	1.026	1.027	1.042
LFR	0.845	0.974	0.535	1.359	1.360	1.391
Makeham	0.288	0.213	0.184	0.452	0.453	0.486

Consistently, our test demonstrates superior performance. Notably, the suggested test, $\hat{\Delta}(0.97)$, was computed with diverse values of s to optimize efficiency across all scenarios, resulting in notably high efficiency. Furthermore, at $s = 0.97$, this test outperformed other alternatives in all instances.

4. Critical Points of the Null Distribution in Monte Carlo Simulation

In the mathematical technique of Monte Carlo simulation, random sampling is employed to predict potential outcomes of events that cannot be precisely determined. Originating during World War II by Stanislaw Ulam and John von Neumann, this method utilizes an anticipated range of values instead of fixed inputs to foresee a series of potential outcomes. By employing a probability distribution, random samples are generated and results computed for each sample, repeated multiple times to create a distribution of plausible conclusions for statistical analysis. To assess the probability of an event occurring through a Monte Carlo simulation, several steps are followed: selecting relevant random variables influencing the event's probability, determining the probability distribution for each variable to generate random samples, analyzing each sample's event frequency, dividing the total samples by iterations, multiplying the result by 100 iteratively to compute the percentage. Subsequently, calculating the percentage mean and standard deviation offers an evaluation of the event's likelihood and the associated uncertainty level.

4.1. Critical points

In statistics, a critical value (C.V.) denotes a specific point within a distribution of a test statistic, determining the possibility of rejecting the null hypothesis. This point is often referred to as the rejection region or crucial zone. Typically, one critical value is used for one-sided tests, while two critical values are utilized for two-sided tests. The preference between the critical value and probability value methods lacks a definitive consensus in statistical literature. Each method presents its own advantages and drawbacks, and the choice often depends on the circumstances and personal preferences. In this phase, the critical sections of the null Monte Carlo distribution are simulated, employing 10,000 size-generated samples with n = 5(5)100. For the confidence levels of 90%, 95%, and 99%, the higher percentile of $\hat{\Delta}(0.97)$ was determined. As indicated in Table 2 and Figure 1, the critical values increased with higher confidence levels and decreased with larger sample sizes, respectively.

Table 2. Critical values of the statistic $\hat{\Delta}(0.97)$.

n	90%	95%	99%
5	1.882110	2.544200	4.238640
10	1.007560	1.267820	1.933870
15	0.754354	0.941814	1.384940
20	0.638263	0.800401	1.112540
25	0.567152	0.692943	0.957504
30	0.496955	0.611205	0.837122
35	0.476944	0.581277	0.779751
40	0.433451	0.533899	0.729413
45	0.396187	0.490734	0.657885
50	0.378519	0.468994	0.632254
55	0.368909	0.448295	0.603413
60	0.343926	0.422245	0.567477
65	0.329967	0.412038	0.566711
70	0.322261	0.394783	0.534692
75	0.310641	0.382725	0.531354
80	0.301035	0.364904	0.494637
85	0.291630	0.362443	0.491624
90	0.279180	0.347682	0.472357
95	0.271664	0.331917	0.449013
100	0.262797	0.319670	0.433857

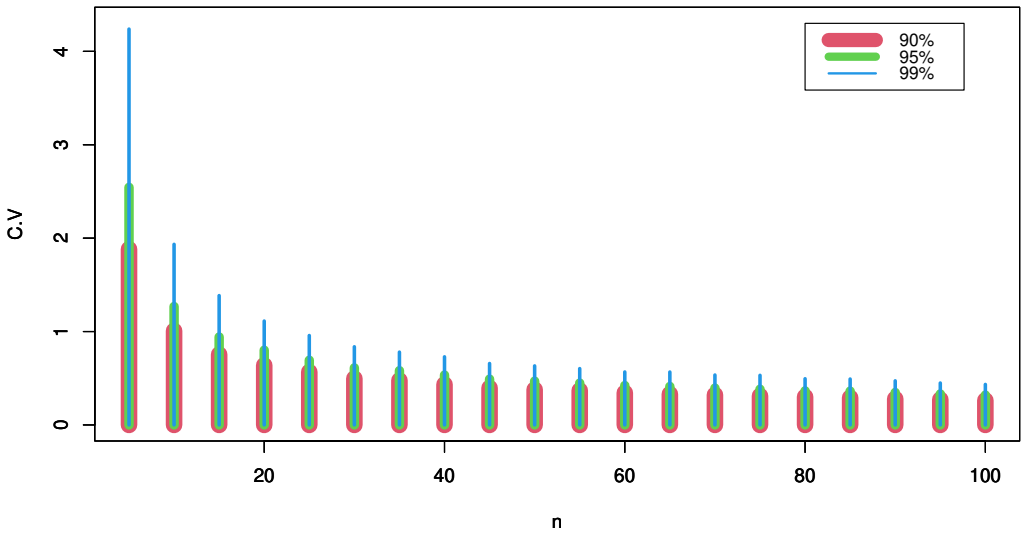

Figure 1. Sample size, confidence levels, and critical values in relation to each other under complete data.

As can be shown in Table 2 and Fig. 1, the critical values decrease with increasing sample numbers and increase with increasing confidence levels.The critical values are rising with rising confidence levels and fall with rising sample sizes, as seen in Table 2 and Fig 1, respectively.

4.2. Test's power estimates $\Delta_n(0.97)$

In statistics, the computations utilized to ascertain the minimum sample size for a study are termed as power estimates. Power represents the probability of correctly rejecting the null hypothesis if it is indeed true. Its key components encompass power itself, significance level, sample size, and the quantity of observations or research participants. To evaluate the effectiveness of the proposed test, the analysis was conducted using the 10,000 samples presented in Table 3 at the $(1-\alpha)\%$ confidence level, with $\alpha = 0.05$. It is assumed that θ when $n = 10, 20$ and 30, respectively holds the accurate values for the Weibull distribution (WD), linear failure rate (LFR), and gamma distribution (GD). The results displayed in Table 3 indicate that the $\Delta_n(0.97)$ test utilized demonstrates adequate power across all other alternatives.

Table 3. Power estimates of $\Delta_n(0.97)$.

n	θ	WD	GD	LFR
10	2	0.9975	0.9989	0.6816
	3	1.0000	0.9999	0.8855
	4	1.0000	1.0000	0.9674
20	2	1.0000	1.0000	0.9876
	3	1.0000	1.0000	0.9995
	4	1.0000	1.0000	1.0000
30	2	1.0000	1.0000	1.0000
	3	1.0000	1.0000	1.0000
	4	1.0000	1.0000	1.0000

5. Testing for Censored Data

To conduct a comparison between H_0 and H_1 using randomly right-censored data, a proposed test statistic is introduced. In scenarios like clinical studies or life-testing models where participants or subjects may be lost (censored) before the trial concludes, this type of censored data often remains the only available information. Here is a more detailed formalization of this hypothetical experiment: Let's consider the verification of n items, with each object's true lifespan denoted as $X_1, X_2, ..., X_n$. Assuming a continuous life distribution F, we allow $X_1, X_2, ..., X_n$ to be independently and identically distributed (i.i.d.). Additionally, let G represent a continuous life distribution, and let $Y_1, Y_2, ..., Y_n$ be (i.i.d.). It's further assumed that both the X's and Y's are independent variables. Within the randomly right-censored model, we observe pairs (Z_j, δ_j), $j = 1, ..., n$, with

$Z_j = \min(X_j, Y_j)$ and

$$\delta_j = \begin{cases} 1, & \text{if } Z_j = X_j \text{ (j-th observation is uncensored)} \\ 0, & \text{if } Z_j = Y_j \text{ (j-th observation is censored)} \end{cases}.$$

The orderd Z's are denoted as $Z_{(0)} = 0 < Z_{(1)} < Z_{(2)} < .... < Z_{(n)}$, and $\delta_{(j)}$ is δ_j corresponding to $Z_{(j)}$. The product limit estimator was suggested by Kaplan and Meier [25] using the censored data (Z_j, δ_j), $j = 1, ..., n$.

$$\overline{F}_n(X) = \prod_{[j:Z(j)\leq X]} \left\{(n-j)/(n-j+1)\right\}^{\delta_{(j)}}, X \in [0, Z_{(n)}].$$

We now suggest the following test statistic to compare $H_0 : \hat{\phi}_c = 0$ with $H_1 : \hat{\phi}_c > 0$ using the randomly right censored data

$$\hat{\phi}_c = \frac{1}{s^2}\mu\phi(s) + \frac{1}{s^3}\phi(s) - \frac{1}{2}\mu\mu_{(2)} - \frac{1}{2s}\mu_{(2)} + \left(\frac{1}{s} + 1\right)\mu^2 - \frac{1}{s^3},$$

where $\phi(s) = \int_0^\infty e^{-sx} dF_n(x)$. To facilitate computation, $\hat{\phi}_c$ could be reformulated as

$$\hat{\phi}_c = \frac{1}{s^2}\Omega\eta + \frac{1}{s^3}\eta - \frac{1}{2}\Omega\Phi - \frac{1}{2s}\Phi + (\frac{1}{s} + 1)\Omega^2 - \frac{1}{s^3},$$

where

$$\Omega = \sum_{k=1}^{n}[\prod_{m=1}^{k-1} C_m^{\delta(m)} \left(Z_{(k)} - Z_{(k-1)}\right)],$$

$$\Phi = 2\sum_{i=1}^{n}[\prod_{v=1}^{i-1} Z_{(i)} C_v^{\delta(v)} \left(Z_{(i)} - Z_{(i-1)}\right)],$$

$$\eta = \sum_{j=1}^{n} e^{-sZ_{(j)}}[\prod_{p=1}^{j-2} C_p^{\delta(p)} - \prod_{p=1}^{j-1} C_p^{\delta(p)}],$$

and

$$dF_n\left(Z_j\right) = \overline{F}_n(Z_{j-1}) - \overline{F}_n(Z_j), c_k = \left[n-k\right]\left[n-k+1\right]^{-1}.$$

To make the test invarient, let

$$\hat{\Delta}_c = \frac{\hat{\phi}_c}{\overline{Z}^3}, \text{ where } \overline{Z} = \sum_{i=1}^{n} \frac{Z_{(i)}}{n}. \tag{12}$$

Table 4 and Figure 2 exhibit the critical percentiles of the $\hat{\Delta}_c$ test corresponding to sample sizes of $n = 10(10)100$. By utilizing the standard exponential distribution and performing 10,000 replications using the Mathematica 12 program, critical values for the null Monte Carlo distribution were derived at $s = 0.97$. As depicted in Figure 2 and detailed in Table 4, the critical values exhibit an upward trend with higher confidence levels and a declining pattern as the sample size increases.

Table 4. The upper percentile of $\hat{\Delta}_c$ with 10000 replications at $s = 0.97$.

n	90%	95%	99%
10	3.24668	7.38013	24.6683
20	1.58340	3.25286	8.38960
30	1.16386	2.38361	5.82690
40	0.88624	1.81084	4.04146
50	0.68573	1.43970	3.43635
60	0.61884	1.30761	3.00585
70	0.52197	1.11054	2.62166
80	0.48741	0.97166	2.21053
90	0.42521	0.90854	1.96633
100	0.39507	0.85163	1.90046

Table 4 illustrates how the critical values rise with increasing confidence levels and fall with larger sample numbers.

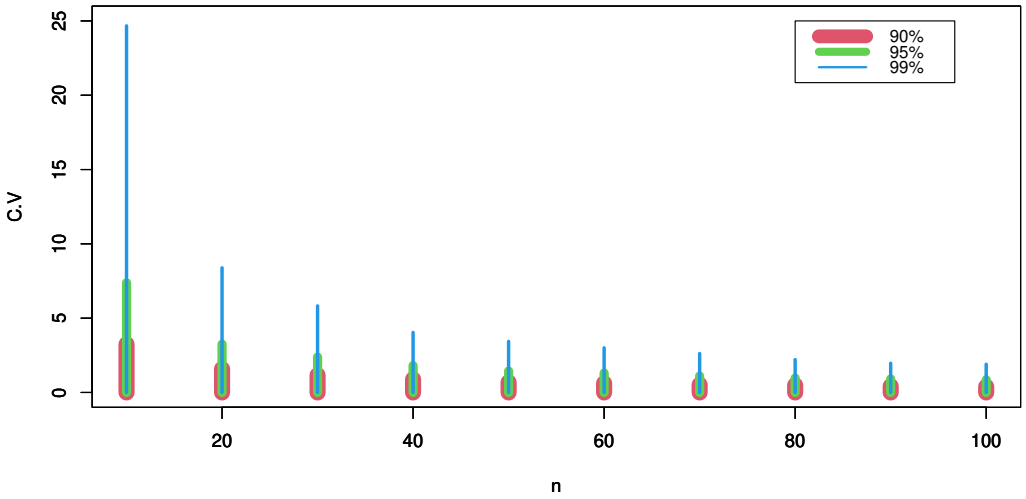

Figure 2. Sample size, confidence levels, and critical values in relation to each other under censored data.

As demonstrated in Table 4 and Figure 2, there is a noticeable trend where the critical values escalate with higher confidence levels and diminish with greater sample sizes.

5.1. Estimates of test power $\Delta_c(s)$

By examining the parameter values of θ at $n = 10, 20$, and 30 across three distinct distributions, say Weibull, LFR, and gamma, using 10,000 samples, the effectiveness of our test was assessed at a significance threshold of $\alpha = 0.05$. The results displayed in

Table 5 indicate that our test, $\Delta_c(0.97)$'s, exhibited commendable power estimates for all alternative scenarios.

Table 5. Power estimates of $\Delta_c(0.97)$.

n	θ	Weibull	LFR	Gamma
10	2	0.9832	0.9975	0.9934
	3	0.9999	0.9995	0.9980
	4	1.0000	1.0000	0.9999
20	2	0.9710	0.9913	0.9836
	3	0.9994	0.9990	0.9945
	4	1.0000	0.9997	0.9986
30	2	0.9698	0.9897	0.9792
	3	0.9988	0.9978	0.9923
	4	1.0000	0.9996	0.9981

6. Applications of Sustainability Data from Censored and Uncensored Observations to Real-World Scenarios

Statistical analysis of censored data can pose challenges due to missing or inadequate data, often necessitating special methods and assumptions. In contrast, unsupervised (or unfiltered) data alleviates these challenges, as it is devoid of such issues, thus streamlining the analysis process.

6.1. Uncensored data

6.1.1. Dataset I: Electrical data

The experimental failure periods, expressed in seconds, for two distinct kinds of electrical insulation subjected to continuous voltage stress, were taken into consideration by Alsadat et al. [26]. Each type of electrical insulation has thirty samples, all of which were examined and documented.

- The initial failure rates for type X are as follows: 0.097, 0.014, 0.03, 0.134, 0.240, 0.084, 0.146, 0.024, 0.045, 0.004, 0.099, 0.277, 0.472, 0.094, 0.023, 0.146, 0.030, 0.031, 0.104, 0.105, 0.036, 0.065, 0.022, 0.098, 0.178, 0.059, 0.014, 0.007, 0.007, 0.286.
- The second type Y's failure rates can be listed as: 0.084, 0.236, 0.315, 0.199, 0.252, 0.103, 0.455, 0.135, 0.348, 0.321, 0.166, 0.04, 0.027, 0.519, 0.017, 0.821, 0.942, 0.27, 0.008, 0.03, 0.177, 0.268, 0.18, 0.796, 0.245, 0.703, 0.045, 0.314, 0.281, 0.652.

Non-parametric plots of types X and Y are shown in Figures 3 and 4, respectively. The behavior of the tested data is discussed and evaluated using these charts. It was observed that both situations exhibit noticeable outlier observations, which causes the data to be

skewed to the right. The shape of the hazard shown in datasets X and Y showed a pattern suggestive of a trend shaped like a bathtub-unimodal failure.

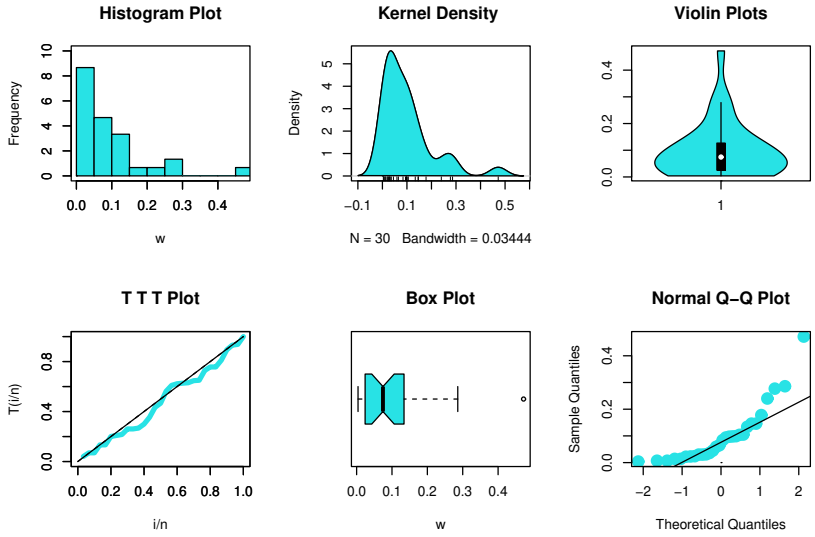

Figure 3. Non-parametric plots for dataset I (type X).

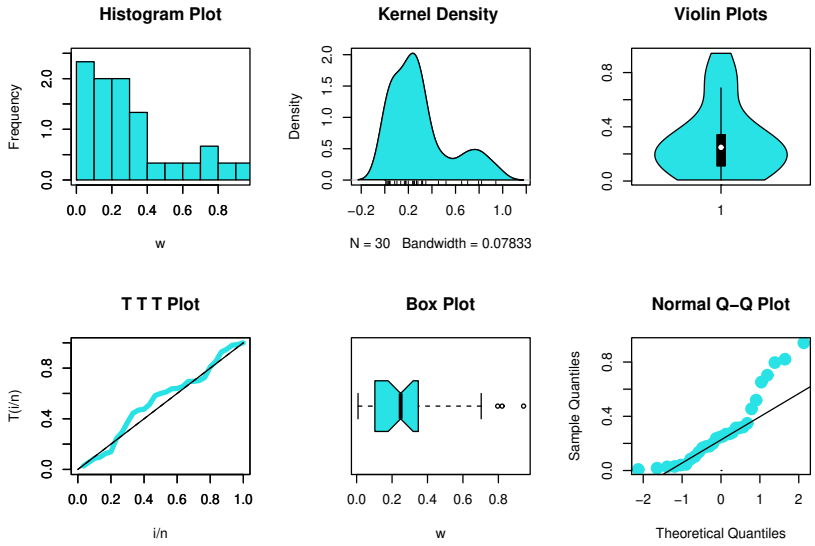

Figure 4. Non-parametric plots for dataset I (type Y).

For data type X, the computed value $\hat{\Delta} = 9.03302$ significantly exceeds the critical threshold indicated in Table 2. At the $\alpha = 0.05$ significance level, the data validates the validity of the $EBUCL$ feature. Additionally, for data type Y, $\hat{\Delta} = 2.66437$ exceeds the crucial threshold shown in Table 2. This implies that rather than exhibiting exponential

development as claimed in H_1, the data collection exhibits an $EBUCL$ feature, which we subsequently accept.

6.1.2. Dataset II: Variations in heights between plants

Investigate the extensively documented Darwin dataset (Fisher [27]), depicting height discrepancies among plants from the same pair cultivated in a shared pot versus those seeded separately. The values in the dataset include 4.9, −6.7, 0.8, 1.6, 2.3, 2.8, 4.1, 1.4, 2.9, 0.6, 5.6, 2.4, 7.5, 6.0, and −4.8. Non-parametric plots were generated in Figure 5 to explore the data's characteristics. It is observed that the data contains outliers, resulting in an asymmetric distribution with a bimodal shape. Additionally, TTT plots reveal a bathtub-shaped hazard.

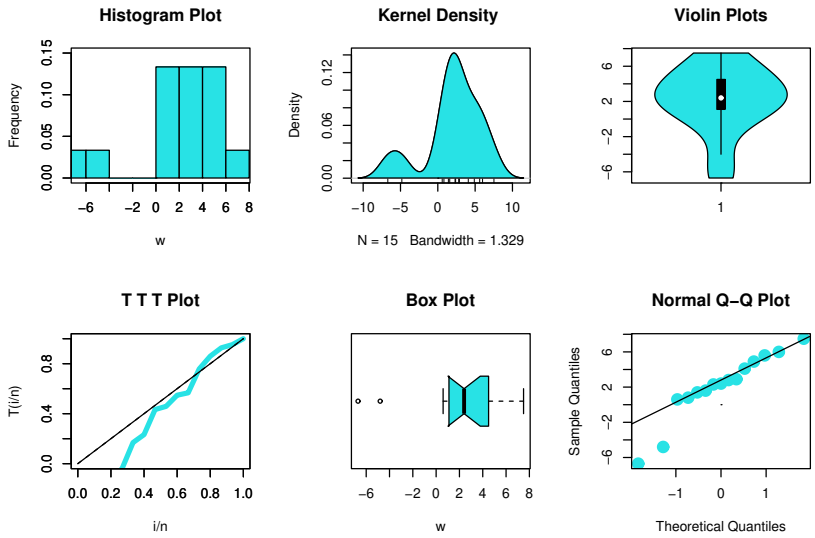

Figure 5. Non-parametric plots for data set II.

In this context, the calculated value, $\hat{\Delta} = 16.4593$, notably surpasses the critical value outlined in Table 2. Such data aligns with the EBUCL characteristic, therefore confirming its validity at the $\alpha = 0.05$ significance level.

6.1.3. Dataset III: Strength of single carbon fibers

This section examined two datasets employed by Kundu and Gupta [28] and presented in Badar and Priest [29]. Set A entails the assessment of single carbon fibers' strength under tension, utilizing gauge lengths of 20 mm, measured in GPA. Set B, on the other hand, involves the evaluation of single carbon fibers' strength, expressed in GPA, after stress testing at gauge lengths of 10 mm. The values in the dataset A include: 1.312,

1.314, 1.479, 1.552, 1.700, 1.803, 1.861, 1.865, 1.944, 1.958, 1.966, 1.997, 2.006, 2.021, 2.027, 2.055, 2.063, 2.098, 2.140, 2.179, 2.224, 2.240, 2.253, 2.270, 2.272, 2.274, 2.301, 2.301, 2.359, 2.382, 2.382, 2.426, 2.434, 2.435, 2.478, 2.490, 2.511, 2.514, 2.535, 2.554, 2.566, 2.570, 2.586, 2.629, 2.633, 2.642, 2.648, 2.684, 2.697, 2.726, 2.770, 2.773, 2.800, 2.809, 2.818, 2.821, 2.848, 2.880, 2.954, 3.012, 3.067, 3.084, 3.090. Where are the values in the dataset B include: 1.901, 2.132, 2.203, 2.228, 2.257, 2.350, 2.361, 2.396, 2.397, 2.445, 2.454, 2.474, 2.518, 2.522, 2.525, 2.532, 2.575, 2.614, 2.616, 2.618, 2.624, 2.659, 2.675, 2.738, 2.740, 2.856, 2.917, 2.928, 2.937, 2.937, 2.977, 2.996, 3.030, 3.125, 3.139, 3.145, 3.220, 3.223, 3.235, 3.243, 3.264, 3.272, 3.294, 3.332, 3.346, 3.377, 3.408, 3.435, 3.493, 3.501, 3.537, 3.554, 3.562, 3.628, 3.852, 3.871, 3.886, 3.971, 4.024, 4.027, 4.225, 4.395, 5.020. Figures 6 and 7 were utilized to create non-parametric plots for an in-depth examination of the data's features. Notably, dataset B displays outliers, in contrast to dataset A. Moreover, TTT plots illustrate a hazard with an increasing shape.

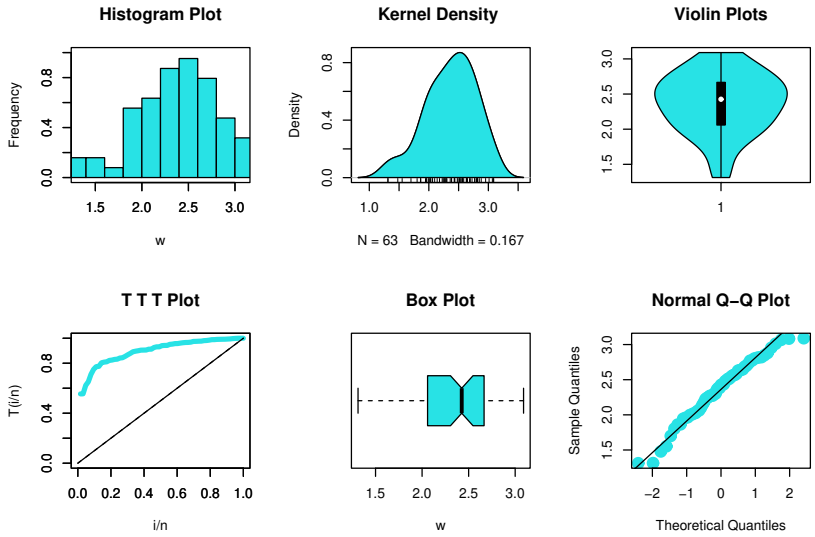

Figure 6. Non-parametric plots for data set III-A.

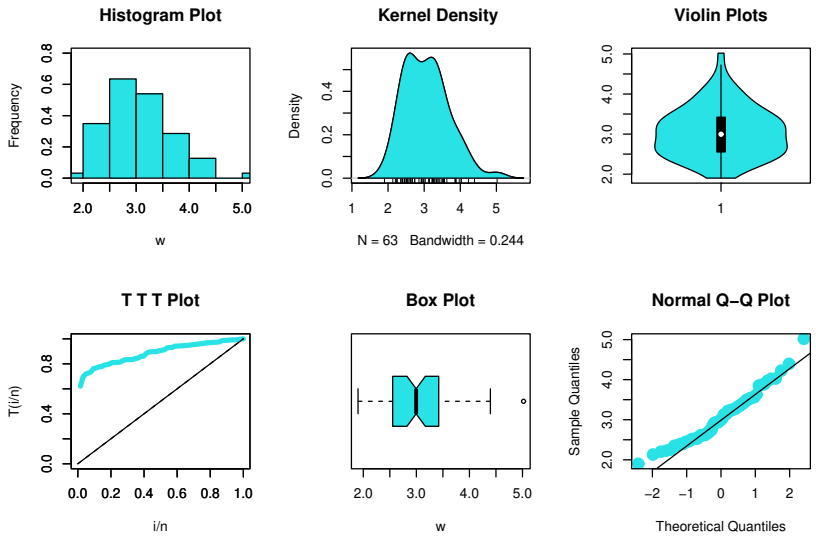

Figure 7. Non-parametric plots for data set III-B.

The observed value of $\hat{\Delta} = 0.0649338$ falls below the critical value specified in Table 2 for dataset A. This implies the presence of noticeable exponential patterns in the data. In contrast, the observed value of $\hat{\Delta} = -0.0608629$ for dataset B deviates from the critical value in Table 2, further highlighting the discernible presence of exponential patterns in the data.

6.1.4. Dataset IV: Tensile strength of fiberglass

The dataset presents outcomes from tests performed at the National Physical Laboratory in England, focusing on the tensile strengths of 1.5 cm glass fibers. This data collection has been addressed by Adepoju et al. [30]. The data can be listed as: 0.55, 0.93, 1.25, 1.36, 1.49, 1.52, 1.58, 1.61, 1.64, 1.68, 1.73, 1.81, 1.04, 1.27, 1.39, 1.49, 1.53, 1.59, 1.61, 1.66, 1.68, 1.76, 1.82, 2.01, 0.77, 1.11, 1.28, 1.42, 1.50, 1.54, 1.60, 1.62, 1.66, 1.69, 1.76, 1.84, 2.24, 0.81, 1.13, 1.29, 1.48, 1.50, 1.55, 1.61, 1.62, 1.66, 1.70, 1.77, 1.84, 0.84, 1.24, 1.30, 1.48, 1.51, 1.55, 1.61, 1.63, 1.67, 1.70, 1.78, 1.89, 0.74, 2.00. Figure 8 is employed to generate non-parametric plots for a thorough exploration of the data's characteristics. Noteworthy is the presence of extreme in dataset. Additionally, the TTT plots depict a hazard exhibiting an increasing shape.

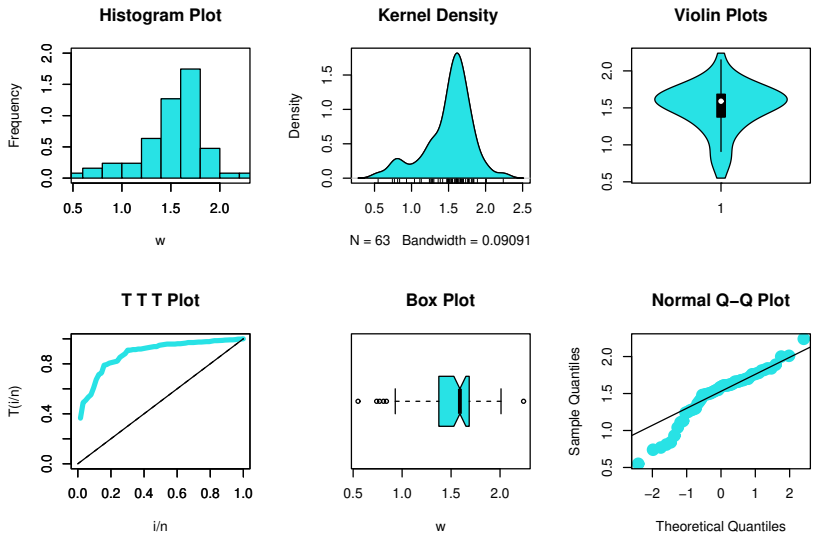

Figure 8. Non-parametric plots for data set IV.

The critical value obtained from Table 2, which stands at $\hat{\Delta} = 0.339959$, exceeds our determined value. Therefore, the evident exponential nature of the data becomes apparent.

6.1.5. Dataset V: Milk produced by SINDI cows

This dataset comprises the cumulative milk production from 107 SINDI race cows since their initial birth. The details can be referenced in Cordeiro and Birto [31]. Specifically, the dataset is as follows: 0.4365, 0.4260, 0.5140, 0.6907, 0.7471, 0.2605, 0.6196, 0.8781, 0.4990, 0.6058, 0.6891, 0.5770, 0.5394, 0.1479, 0.2356, 0.6012, 0.1525, 0.5483, 0.6927, 0.7261, 0.3323, 0.0671, 0.2361, 0.4800, 0.5707, 0.7131, 0.5853, 0.6768, 0.5350, 0.4151, 0.6789, 0.4576, 0.3259, 0.2303, 0.7687, 0.4371, 0.3383, 0.6114, 0.3480, 0.4564, 0.7804, 0.3406, 0.4823, 0.5912, 0.5744, 0.5481, 0.1131, 0.7290, 0.0168, 0.5529, 0.4530, 0.3891, 0.4752, 0.3134, 0.3175, 0.1167, 0.6750, 0.5113, 0.5447, 0.4143, 0.5627, 0.5150, 0.0776, 0.3945, 0.4553, 0.4470, 0.5285, 0.5232, 0.6465, 0.0650, 0.8492, 0.8147, 0.3627, 0.3906, 0.4438, 0.4612, 0.3188, 0.2160, 0.6707, 0.6220, 0.5629, 0.4675, 0.6844, 0.3413, 0.4332, 0.0854, 0.3821, 0.4694, 0.3635, 0.4111, 0.5349, 0.3751, 0.1546, 0.4517, 0.2681, 0.4049, 0.5553, 0.5878, 0.4741, 0.3598, 0.7629, 0.5941, 0.6174, 0.6860, 0.0609, 0.6488, 0.2747. Figure 9 is utilized to create non-parametric plots for a comprehensive analysis of the data's characteristics. Notably, there are some extremes observed in the dataset. Furthermore,

the TTT plots illustrate a hazard with an increasing shape.

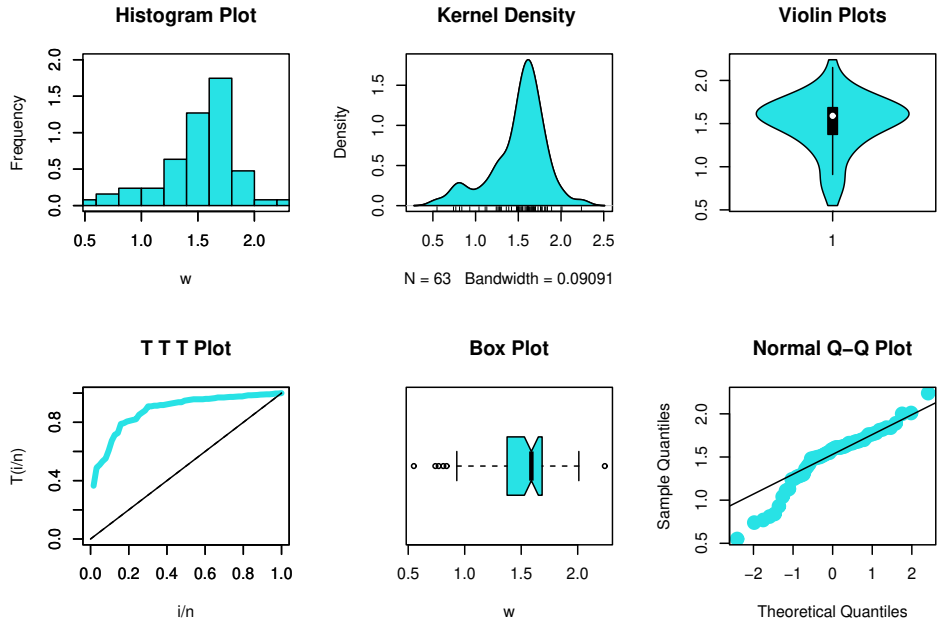

Figure 9. Non-parametric plots for data set V.

The critical value depicted in Table 2 was found to be exceeded by $\hat{\Delta} = 1.82338$. Accordingly, our agreement aligns with hypothesis H_1, suggesting that the data collection is characterized by $EBUCL$ rather than exponential growth.

6.2. Censored data

6.2.1. Dataset VI: Incurable lung cancer

As reported by Lagakos and Williams ([32]) and Lee and Wolfe ([33]), out of 61 patients treated with cyclophosphamide for incurable lung cancer, the following statistics were observed: 33 patients had unfiltered observations, while 28 patients had their treatment stopped due to deteriorating health, leading to censored observations. Observational censorship: 0.14, 0.14, 0.29, 0.43, 0.57, 0.57, 1.86, 3.00, 3.00, 3.29, 3.29, 6.00, 6.00, 6.14, 8.71, 10.57, 11.86, 15.57, 16.57, 17.29, 18.71, 21.29, 23.86, 26.00, 27.57, 32.14, 33.14, 47.29. Uncensored observations: 0.43, 2.86, 3.14, 3.14, 3.43, 3.43, 3.71, 3.86, 6.14, 6.86, 9.00, 9.43, 10.71, 10.86, 11.14, 13.00, 14.43, 15.71, 18.43, 18.57, 20.71, 29.14, 29.71, 40.57, 48.57, 49.43, 53.86, 61.86, 66.57, 68.71, 68.96, 72.86, 72.86. When considering all survival data, including both censored and uncensored observations, our finding, $\Delta_c(0.97) = -2.67235 \times 10^{49}$, falls below the critical threshold indicated in Table 4. Hence, the exponential pattern within the data becomes evident.

6.2.2. Dataset VII: Tongue cancer patients

The dataset presents the estimated time of death (in weeks) for tongue cancer patients with aneuploidy DNA profiles. Previous references utilizing this data include Sickle-Santanello et al. [34] and Klein and Moeschaberger [35]. The dataset contains 51 observations: 1, 3, 3, 4, 10, 13, 16, 16, 24, 28, 30, 30, 32, 41, 51, 61+, 65, 67, 72, 73, 74+, 77, 79+, 80+, 81+, 87+, 87+, 89+, 91, 93+, 96, 97+, 100, 101+, 104, 104+, 109+, 120+, 150+, 131+, 157, 167, 13, 231+, 240+, 24, 27, 70, 88+, 108+, 400. The result of $\Delta_c(0.97) = -3.35085 \times 10^{20}$ is derived, falling below the critical threshold detailed in Table 4. Hence, this supports the null hypothesis regarding the exponential characteristic, leading to the rejection of the alternative hypothesis of EBUCL.

7. Conclusion

This study provided a comprehensive examination of the exponential distribution, a fundamental concept in statistical theory with wide applications in reliability theory, life testing, and stochastic processes. The research focused on the development of innovative nonparametric testing techniques to assess whether data conform to the properties of the exponential distribution and the EBUCL class. Both complete and censored datasets were thoroughly analyzed, and the study demonstrated the asymptotic normality of the proposed test. Additionally, the paper calculated upper percentile values for the test statistics using Monte Carlo simulations, and evaluated the power of the test against alternative distributions, including the LFR, Gamma, and Weibull distributions. The results were further validated through the calculation of Pitman's asymptotic relative efficiencies and applied to real-world datasets, confirming the test's practical utility and reliability in various fields. The findings have important implications for reliability engineering, where the exponential distribution is widely used to model constant failure rates, allowing engineers to effectively schedule maintenance and predict potential system failures. This study also highlighted the relevance of exponentiality testing in healthcare, where it plays a crucial role in understanding disease trajectories, evaluating interventions, and forecasting public health outcomes such as epidemic frequencies and vaccine efficacy. By providing a rigorous statistical framework for testing exponentiality and examining the reliability of systems in both engineering and healthcare, this research contributes valuable insights that can guide decision-making, enhance predictive models, and foster more effective maintenance and healthcare planning strategies. The study emphasizes the importance of exponentiality testing in real-world applications and lays the groundwork for future research that could expand these methodologies across other sectors of applied mathematics and reliability theory.

Acknowledgements

This project was supported by the deanship of scientific research at Prince Sattam bin Abdulaziz University, Al-Kharj, Saudi Arabia. This study is supported via funding from

Prince Sattam bin Abdulaziz University project number (PSAU/2025/R/1446).

Data Availability: Data are contained within the article.
Conflicts of interest: The authors declare no conflicts of interest.

Acknowledgements

References

[1] R. M. EL-Sagheer, M. A. W. Mahmoud, and W. B. H. Etman. Characterizations and testing hypotheses for NBRUL-t_0 class of life distributions. Journal of Statistical Theory and Practice, 16(2):31, 2022.

[2] J. Navarro and F. Pellerey. Preservation of ILR and IFR aging classes in sums of dependent random variables. Applied Stochastic Models in Business and Industry, 38(2):240–261, 2022.

[3] S. Ghosh and M. Mitra. A new test for exponentiality against HNBUE alternatives. Communications in Statistics - Theory and Methods, 49(1):27–43, 2020.

[4] M. E. Bakr and A. A. Al-Babtain. Non-parametric hypothesis testing for unknown aged class of life distribution using real medical data. Axioms, 12:369, 2023.

[5] H. Alqifar, M. S. Eliwa, W. B. H. Etman, M. El-Morshedy, L. A. Al-Essa, and R. M. EL-Sagheer. Reliability class testing and hypothesis specification: NBRULC-t_0 characterizations with applications for medical and engineering data modeling. Axioms, 12(5):414, 2023.

[6] M. C. Bryson and M. M. Siddiqui. Some criteria for aging. Journal of the American Statistical Association, 64(328):1472–1483, 1969.

[7] R. E. Barlow and F. Proschan. Statistical theory of reliability and life testing. To Begin With, Silver Spring, MD, 1981.

[8] M. El-Morshedy, A. Al-Bossly, R. M. EL-Sagheer, B. Almohaimeed, W. B. H. Etman, and M. S. Eliwa. A moment inequality for the NBRULC class: statistical properties with applications to model asymmetric data. Symmetry, 14:2353, 2022.

[9] A. M. Gadallah, B. I. Mohammed, A. A. Al-Babtain, S. K. Khosa, M. Kilai, M. Yusuf, and M. E. Bakr. Modeling various survival distributions using a nonparametric hypothesis testing based on Laplace transform approach with some real applications. Computational and Mathematical Methods in Medicine, Article ID 5075716:1–8, 2022.

[10] M. M. M. Mansour. Assessing treatment methods via testing exponential property for clinical data. Journal of Statistics Applications & Probability, 11(1):109–113, 2022.

[11] B. Klefsjo. The HNBUE and HNWUE classes of life distributions. Naval Research Logistics, 29(2):331–344, 1982.

[12] Y. Kumazawa. A class of tests statistics for testing whether new is better than used. Communications in Statistics - Theory and Methods, 12:311–321, 1983.

[13] S. E. Abu-Youssef, Nahed S. A. Ali, and M. E. Bakr. Used better than aged in mgf ordering class of life distribution with application of hypothesis testing. Journal of Statistics Applications & Probability Letters, 7(1):23–32, 2020.

[14] M. A. W. Mahmoud and M. M. M. Mansour. Non parametric test for testing exponentiality against exponential better than used in Laplace transform order. Journal of Statistics Applications & Probability, 8(1):1–9, 2019.
[15] M. E. Bakr. Statistical modeling for some real applications in reliability analysis using non-parametric hypothesis testing. Symmetry, 15:1735, 2023.
[16] S. A. Qaid, S. E. Abu-Youssef, and M. M. M. Mansour. Formulating an efficient statistical test using the goodness of fit approach with applications to real-life data. Journal of Statistics Applications & Probability, 13(1):409–418, 2024.
[17] Wen-Qi Duan, Z. Khan, M. Gulistan, and A. Khurshid. Neutrosophic exponential distribution: modeling and applications for complex data analysis. Complexity, Article ID 5970613:1–8, 2021.
[18] J. W. Poston. Encyclopedia of Physical Science and Technology (Third Edition), Academic Press, 603–650, 2003.
[19] J. Beckers, W. W. Stoffels, T. Ockenga, M. Wolter, and H. Kersten. Microparticles in a RF plasma under hyper gravity conditions. IEEE International Conference on Plasma Science - Abstracts, San Diego, CA, USA, pp. 1–1, 2009.
[20] L. Tomy, M. Jose, and G. Veena. A review on recent generalizations of exponential distribution. Biometrics & Biostatistics International Journal, 9(4):152–156, 2020.
[21] I. I. El-Batal. The EBU and EWU classes of life distribution. Journal of the Egyptian Mathematical Society, 18(1):59–80, 2002.
[22] A. J. Lee. U-Statistics, Marcel Dekker, New York, 1989.
[23] W. B. H. Etman, M. S. Eliwa, H. Alqifar, M. El-Morshedy, L. A. Al-Essa, and R. M. EL-Sagheer. The NBRULC reliability class: Mathematical theory and goodness-of-fit testing with applications to asymmetric censored and uncensored data. Mathematics, 11:2805, 2023.
[24] A. A. Abdel Aziz. On testing exponentiality against RNBRUE alternatives. Applied Mathematical Sciences, 35:1725–1736, 2007.
[25] E. L. Kaplan and P. Meier. Nonparametric estimation from incomplete observation. Journal of the American Statistical Association, 53(282):457–481, 1958.
[26] N. Alsadat, E. M. Almetwally, M. Elgarhy, H. Ahmad, and G. A. Marei. Bayesian and non-Bayesian analysis with MCMC algorithm of stress-strength for a new two parameters lifetime model with applications. AIP Advances, 13:095203, 2023.
[27] R. A. Fisher. The Design of Experiments, Eighth Edition, Oliver & Boyd, Edinburgh, 1966.
[28] D. Kundu and R. D. Gupta. Estimation of P[Y<X] for Weibull distributions. IEEE Transactions on Reliability, 55(2):270–280, 2006.
[29] M. G. Bader and A. M. Priest. Statistical aspects of fibre and bundle strength in hybrid composites. In: Hayashi, T., Kawata, K. and Umekawa, S., Eds., Progress in Science and Engineering of Composites, ICCM-IV, Tokyo, pp. 1129–1136, 1982.
[30] K. A. Adepoju, A. U. Chukwu, and M. Wang. The beta power exponential distribution. Journal of Statistical Science and Application, 2:37–46, 2014.
[31] G. M. Cordeiro and R. S. Brito. The beta power distribution. Brazilian Journal of Probability and Statistics, 26(1):88–112, 2012.

[32] S. W. Lagakos and J. S. Williams. Models for censored survival analysis: a cone class of variable-sum models. Biometrika, 65(1):181–189, 1978.

[33] S. Y. Lee and R. A. Wolfe. A simple test for independent censoring under the proportional hazards model. Biometrics, 54(3):1176–1182, 1998.

[34] B. J. Sickle-Santanello, W. B. Farrar, J. K. DeCenzo, S. Keyhani-Rofagha, J. Klein, D. Pearl, H. Laufman, and R. V. O. Toole. Technical and statistical improvements for flow cytometric DNA analysis of paraffin-embedded tissue. Cytometry, 9(6):594–599, 1988.

[35] J. P. Klein and M. L. Moeschberger. Survival Analysis: Techniques for Censored and Truncated Data, 2nd Edition, Springer, New York, USA, 2003.